Int J Clin Exp Pathol 2014;7(8):4645-4660
www.ijcep.com /ISSN:1936-2625/IJCEP0001186

Original Article

Proteomic analysis of immature rat pups brain in response to hypoxia and ischemia challenge

Li-Jun Yang, Dong-Qing Ma, Hong Cui

Department of Pediatrics, Beijing Friendship Hospital, Capital Medical University, Beijing, China

Received June 23, 2014; Accepted August 2, 2014; Epub July 15, 2014; Published August 1, 2014

Abstract: Hypoxia and ischemia significantly affects perinatal brain development, even worse in preterm infants. However, the details of the mechanism leading to permanent brain damage after hypoxia-ischemia attack have not been fully elucidated. Proteomics could provide insight into the potential mechanism and help to promote the clinical treatment. In this study, quantitative analysis was performed 24 hours after hypoxia-ischemia using liquid-chromatography mass spectrometry coupled to label-free analysis. Compared to control, 193 proteins were present only in hypoxic-ischemic group. In addition, 34 proteins were more than 2 folds up-regulated and 14 proteins were more than 2 folds down-regulated in hypoxia-ischemia group. Gene Ontology database showed that the majority of differentially expressed proteins comprised mitochondrial proteins et al. Molecular function analysis revealed that the majority of proteins were involved in ion binding et al. Biological process analysis showed that the majority of proteins were involved in response to organic substance et al. STRING 9.0 software analysis were used to explore the complex interactions existed among the proteins. Western blot were used to verify the fold changes of some proteins-microtubule-associated protein 2 and microtubule-associated protein tau. This novel study performed a full-scale screening of the proteomics research in hypoxic-ischemic brain damage of immature rat.

Keywords: Hypoxia, ischemia, preterm, proteomics

Introduction

Hypoxic-ischemic brain damage (HIBD) refers to fetal/neonatal brain damage caused by partial or complete cerebral hypoxia, cerebral blood flow reduction or suspension. HIBD is a major cause of acute deaths and chronic nervous system damage. Major sequelae of HIBD include long-term neurological disturbances such as cerebral palsy, mental retardation, seizure disorders and motor/cognitive disabilities [1-3]. However, neonatal neuroprotection for hypoxic ischemic brain damage remains elusive. ypothermia improves both survival and the neurologic outcomes of those who survive, but the effect is also limited. In recent years, people are constantly trying new treatments in both cell culture and animal models to HIBD, such as erythropoietin [4-6] and isoflurane [7-10]. But drug and treatments can be used in clinical is still limited to date. Therefore, it is very important to full elucidate the physiopathology of HIBD. A large number of studies show hypoxic-ischemic (H-I) injuries develop in two phases: the ischemic phase and the reperfusion phase [11, 12]. The first phase is dominated by ATP depletion, anaerobic glycolysis and metabolic acidosis and the second phase is dominated by reactive oxygen species (ROS) generation and thus triggers a cascade of chain reactions [13-15]. All these biochemical events cause cells disintegration (death of neuron and glial cells) and alterations in cell ultrastructure, blood-brain barrier (BBB) integrity disrupting, adhesins and chemokines releases and ultimately lead to brain dysfunction. Furthermore, immature brain, which is low maturity and higher likelihood of low perfusion, is more sensitive and vulnerable to all these stimuli and give rise to more serious consequences. However, the details of the mechanism leading to permanent brain damage induced by hypoxia-ischemia have not yet been elucidated. Proteomics can analyze protein expression in specific circumstances such as the formation of hypoxic-ischemic brain damage at the overall level and thus

could provide insight into the potential mechanism. Furthermore, fully elucidated details in brain damage after hypoxia and ischemia attack may allow development of protective therapies. Brain damage following hypoxic-ischemic insult is a complex process evolving over hours to days, which provides a unique window of opportunity for neuroprotective treatment interventions. Recently, therapeutic measures of HIBD are investigated in clinical as well as animal studies, which aim at a further extension of the therapeutic window to days [16].

In this study, we established hypoxia-ischemia brain damage using SD neonatal rats at the 3rd postnatal day (P3) to mimics hypoxic-ischemic event in preterm infants, brain development of P3 SD rats present similar to that of human preterm infants between 24 to 28 weeks of gestation [17, 18]. Therefore, we performed our proteomic analysis one day after induction of HI, at postnatal day P4. We employed label-free quantitative shotgun proteomic methods [19] to make a global comparison of proteins of healthy brain tissue against those brain tissues from hypoxic-ischemic insult in rats. We focused our analysis on the total area of brain tissue affected by the hypoxic-ischemic insult. The overall level of protein expression is considered to be important regulators during HI injury and subsequent regenerative procedure, therefore, is also a potential therapeutic target protein molecules.

Materials and methods

Animals and animal model preparation

Three-day-old neonatal Sprague-Dawley rats (excluding male and female, weighing 8-10 g) were from the Beijing Vital River Laboratory Animal Technology Limited Company [SCXK (Beijing) 2007-0001] breastfeeding by their mother. Rearing conditions were as follows: exposure time: dark time = 12 h: 12 h, temperature: 24°C, Humidity: 40%. A total of 22 neonatal rats were equally and randomly assigned to control group and hypoxia-ischemia group.

The experiment was approved by the University Animal Ethics Committee according to the local government legislation. Briefly, 3-day-old neonatal Sprague-Dawley rats underwent unilateral ligation of the left common carotid artery via a midline neck incision after anesthesia with 0.2 mL of Ether in an airtight box for 1 minute. After that, they were returned to their mother for nursing for 1 hour until they regained normal movement. The rats were subsequently placed in a hypoxic chamber of 8% O_2+92% N_2 maintained at 37°C for 90 minutes to create hypoxia-ischemia brain damage [20]. One day after hypoxia-ischemia treatment, the brain tissue of control group and hypoxia-ischemia group were obtained. Three brains of each group were fixed in 4% formalin for HE staining and eight brains of each group were kept in -80°C refrigerator for further analysis (5 each for label-free quantitative shotgun proteomic analysis and 3 each for western blot analysis).

Protein extraction and digestion

For the differential proteome study, brain tissues of P4 rats undergoing HI at P3 were investigated. Frozen tissue sample was transferred to a cooled mortar with liquid nitrogen to grind to a fine powder. After re-dissolved in 8 M UA buffer (8 M Urea, 150 mM TrisHCl pH 8.0), depicting 1 μL to determine the protein concentration.

Took 100 μg from each sample, added 2 μg Lys-C and incubated for 3 hours at room temperature. Adding 25 mM NH_4HCO_3 to dilute urea concentration to 1.5 M and then added 2 μg trypsin, incubated in 37°C for 20 hours. Then proteins were prepared for examination of 2D-LC-MS/MS analysis.

2D-LC-MS/MS analysis of hydrolysates and label-free analysis

Five μg hydrolysates of each sample were taken to conduct the 2D-LC-MS/MS analysis. Using nano-flow liquid system EASY-nLC1000 HPLC to separate the hydrosysates. Liquid phase solution A was 0.1% formic acid aqueous acetonitrile (acetonitrile was 2%) and liquid phase solution B was 0.1% formic acid aqueous acetonitrile (acetonitrile was 84%). Thermo EASY column SC200 150 μm × 100 mm (RP-C18) was balanced by 100% solution A. Samples were loaded to the Thermo EASY column SC001 traps 150 μm × 20 mm (RP-C18) by autosampler, and then separated by column chromatography, with a flow rate of 400 nl/min. Related phase gradients were as follows: from 0 minute to 100 minutes, the linear gradient of solution B was from 0% to 45%; from 100 minutes to

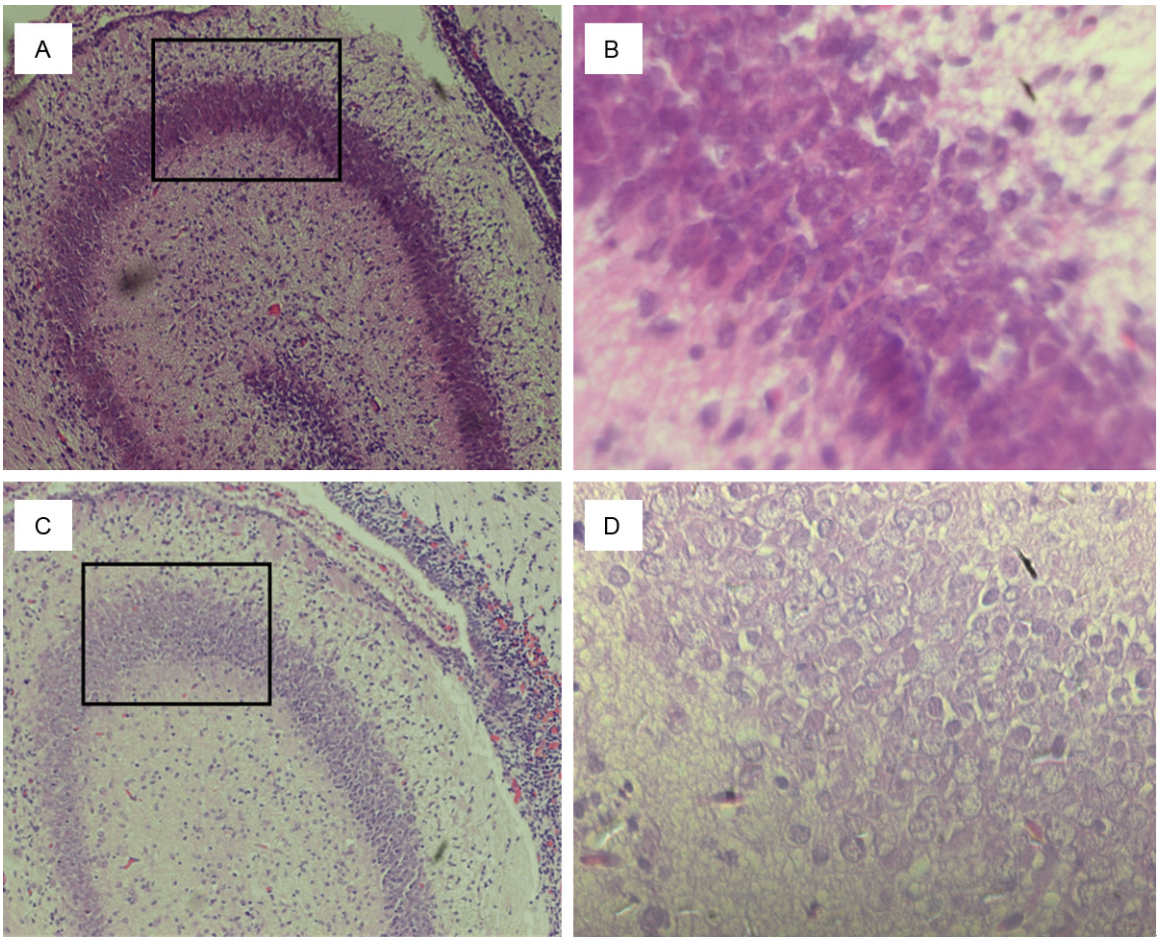

Figure 1. Establishment of hypoxia ischemia brain damage model. A, B. Control group. A. 100 ×, B. 400 ×, cell nucleus showed normal morphology; C, D. Hypoxia ischemia group. C. 100 ×, D. 400 ×, cell nucleus showed fragmentation and dissolution.

108 minutes, linear gradient of solution B was from 45% to 100%; from 108 minutes to 120 minutes, the linear gradient of solution B was maintained at 100%. Hydrolyzates after separation by capillary liquid chromatography were identified by mass spectrum using Q-Exactive mass spectrometer (Thermo Finnigan). The total time was 120 min, detection method was positive ion and precursor ion scan range was 300-1800 m/z. The polypeptides and polypeptide fragments of the mass-charge ratio collected in accordance with the following methods: 10 pieces Atlas (MS2 scan, HCD) were collected after each full scan. The resolution of MS1 at M/Z 200 is 70,000 and the resolution of MS2 at M/Z 200 is 17,500.

The original LC-MS/MS file was imported to Maxquant software (version 1.3.0.5) for Label-free analysis, with the database of Swiss-Prot Rat (2010-04 edition of 3648 entries). The peptides were constrained to be tryptic and up to two missed cleavages were allowed. Carbamidomethylation of cysteines was treated as a fixed modification, whereas oxidation of methionine residues and acetylation of protein N-term were considered as variable modifications. Main search ppm was 6 and MS/MS tolerance ppm was 20, respectively. The false discovery rate (FDR) of peptide and protein were both 0.05.

Cellular component, molecular function and biological process of identified proteins were performed with the tools on DAVID Bioinformatics Resources 2011 (http://david.abcc.ncifcrf.gov/). The association between the most changed proteins was analyzed by the STRING 9.0 software-Known and Predicted Protein-Protein Interactions.

Table 1. Identification of down-regulated proteins (≥2-fold) in HE group versus control

ACC	DESC	Fold change	Molecular weight	PI
Q9QXQ0	Alpha-actinin-4	-101.1	104915.02	5.27
P69897	Tubulin beta-2B chain	-6.8	49670.82	4.78
P46462	Transitional endoplasmic reticulum ATPase	-4.0	89217.64	5.14
P85125	Polymerase I and transcript release factor	-4.0	43908.57	5.42
Q7TP52	Carboxymethylenebutenolidase homolog	-3.6	27771.67	6.26
O55171	Acyl-coenzyme A thioesterase 2, mitochondrial	-3.6	45121.88	6.30
P14668	Annexin A5	-2.8	35613.32	4.91
P19804	Nucleoside diphosphate kinase B	-2.4	17151.79	7.12
P01835	Ig kappa chain C region, B allele	-2.4		
P27605	Hypoxanthine-guanine phosphoribosyltransferase	-2.4	24346.05	6.06
Q62651	Delta (3,5)-Delta (2, 4)-dienoyl-CoA isomerase, mitochondrial	-2.3	32474.24	6.26
P07895	Superoxide dismutase [Mn], mitochondrial	-2.2	22291.29	7.94
P85834	Elongation factor Tu, mitochondrial	-2.1	44984.90	6.20
Q9Z0V6	Thioredoxin-dependent peroxide reductase, mitochondrial	-2.0	21649.69	5.81

Statistical and bioinformatic analysis of perseus

Put the results from Maxquant to the software of Perseus for further analysis. Perseus software version number is 1.2.0.17. In this study, proteins more than 2-fold increased or decreased was cut-off to distinguish changes and analyze. Data are showed as mean ± SEM. Comparisons of quantitative data were analyzed using the two-tail Student's t-test. Statistical significance was set at $P<0.05$.

Western blot analysis

Western Blot analysis was performed on randomly selected brain tissue of HI group (n = 3) and control group (n = 3). Firstly, precooling RIPA protein extraction reagent, added in protease inhibitor cocktail (Roche) and homogenated, incubated on ice for 20 min and centrifuged at 13000 rpm (4°C) for 20 min to get protein. Using BCA protein assay to determine the protein concentration. Adjusted the protein concentration of the sample to a final concentration of 3.5 μg/μL, added 5 × protein sample buffer and incubated at 95°C for 5 min. According to the molecular weight of the protein of interest, we prepared 8% separating gel to separate microtubule-associated protein 2(MAP2) and 10% separating gel to separate microtubule-associated protein tau (Tau). In brief, 70 μg of each protein sample were loaded and the lectrophoresis conditions were as follows: stacking gel 90 V/20 min; separating gel 120 V (through pre-stained protein marker to determine the electrophoretic stop time). The proteins were transferred to a polyvinylidene fluoride (PVDF) membrane. The membranes were completely immersed in 5% BSA-TBST and incubated on horizontal shaker 1 h (RT) to block nonspecific binding sites. After that, membranes were incubated with primary antibodies diluted in blocking reagent overnight at 4°C. After three times washing, the membranes were incubated with horse-radish-peroxidase-conjugated secondary antibodies for 40 min at room temperature. ECL was added to PVDF membrane and reacted for 3-5 min; film exposure: 10 s-5 min (exposure time with different light intensity adjustment). Primary antibodies were used as follows: MAP2 (1:200, Santa Cruz, Texas, USA), Tau (A-12) (1:200, Santa Cruz, Texas, USA), β-actin (1:1000, Zhongshan Golden Bridge Bio-technology, Beijing, China).

Results

Model of perinatal hypoxic-ischemic brain damage

Twenty-four hours after hypoxia-ischemia processing, brain tissue of both control group and hypoxia-ischemia group were obtained and fixed for frozen sections. Then HE staining was performed in both groups to determine the effect of hypoxia and ischemia on brain tissue. Results showed more karyorrhexis and karyopyknosis in cells in the hypoxia/ischemia group compared with the control group (**Figure 1**),

Table 2. Identification of up-regulated proteins (≥2-fold) in HE group versus control

ACC	DESC	Fold change	Molecular weight	PI
Q9R063	Peroxiredoxin-5, mitochondrial	2.0	17034.73	6.73
P11517	Hemoglobin subunit beta-2	2.0	15851.24	8.91
P14480	Fibrinogen beta chain	2.1	50671.00	7.94
P62919	60 S ribosomal protein L8	2.1	27893.46	11.04
Q01205	Dihydrolipoyllysine-residue succinyltransferase component of 2-oxoglutarate dehydrogenase complex, mitochondrial	2.1	41467.69	5.89
Q07936	Annexin A2	2.1	38547.05	7.53
Q63362	NADH dehydrogenase [ubiquinone] 1 alpha subcomplex subunit 5	2.2	13280.59	7.07
P56741	Myosin-binding protein C, cardiac-type (Fragment)	2.2	140761.97	6.13
Q68FX0	Isocitrate dehydrogenase [NAD] subunit beta, mitochondrial	2.2	38787.76	7.82
P27139	Carbonic anhydrase 2	2.3	28982.62	6.88
P31044	Phosphatidylethanolamine-binding protein 1	2.3	20670.20	5.48
P26772	10 kDa heat shock protein, mitochondrial	2.3	10770.47	8.91
P29419	ATP synthase subunit e, mitochondrial	2.4	8123.46	9.35
P21913	Succinate dehydrogenase [ubiquinone] iron-sulfur subunit, mitochondrial	2.4	28724.27	8.78
P48037	Annexin A6	2.4	75622.96	5.38
P63102	14-3-3 protein zeta/delta	2.4	27771.14	4.73
P15651	Short-chain specific acyl-CoA dehydrogenase, mitochondrial	2.5	42187.33	6.38
P06685	Sodium/potassium-transporting ATPase subunit alpha-1	2.5	112581.67	5.27
P14604	Enoyl-CoA hydratase, mitochondrial	2.6	28287.52	6.41
P02680	Fibrinogen gamma chain	2.6	47803.28	5.53
P62963	Profilin-1	2.7	14826.02	8.50
O88767	Protein DJ-1	2.7	19974.17	6.32
P35435	ATP synthase subunit gamma, mitochondrial	2.7	30190.70	8.87
P81155	*Voltage-dependent anion-selective channel protein 2*	2.9	31745.82	7.44
P39069	Adenylate kinase isoenzyme 1	3.6	21583.76	7.66
Q4V8F9	Hydroxysteroid dehydrogenase-like protein 2	3.6	58343.94	5.85
P24090	Alpha-2-HS-glycoprotein	3.6	35929.80	5.95
P11762	Galectin-1	3.7	14725.65	5.09
Q9QX79	Fetuin-B	3.8	39731.22	6.50
P41565	Isocitrate dehydrogenase [NAD] subunit gamma, mitochondrial	3.8	38740.45	8.66
P14046	Alpha-1-inhibitor 3	3.9	161078.03	5.67
P06761	78 kDa glucose-regulated protein	4.4	70474.59	5.01
P51886	Lumican	6.7	36485.83	6.01
Q9Z1P2	Alpha-actinin-1	8.8	102960.33	5.23

which suggested that hypoxia and ischemia model were successfully established and could be used for further analysis.

Label-free quantitative shotgun data and protein identification

To detect and compare the differential proteins involved in the hypoxia-ischemia procedure, we used label-free quantitative shotgun proteomic method. Interestingly, 410 proteins were differentially expressed with 241 proteins displaying more than 2-fold difference when comparing the HI group and the control group. Of these, 14 protein were more than 2-fold down-regulated (**Table 1**), 34 protein were more than 2-fold up-regulated (**Table 2**) in hypoxia-ischemia group and 193 proteins were present only in hypoxia-ischemia group (**Table 3**), determined by liquid chromatography-mass spectrometry/mass spectrometry. Classification of these proteins using Gene Ontology database showed that the majority of differentially expressed proteins comprised mitochondrial proteins, plasma membrane proteins and non-membrane-bounded organelle et al. (**Figure 2**). DAVID classification of proteins by molecular function revealed that the majority of proteins were involved in ion binding, metal ion binding, cation binding and nucleotide binding (transcription factor) (**Figure 3**). DAVID classification of proteins by biological process showed that the majority of proteins

Table 3. Identification of proteins only expressed in HE group versus control

ACC	DESC	Molecular weight	PI
P02401	60S acidic ribosomal protein P2	11691.96	4.40
P02767	Transthyretin	13598.19	5.77
P04762	Catalase	59626.01	7.15
P04785	Protein disulfide-isomerase	54982.89	4.77
P05508	NADH-ubiquinone oxidoreductase chain 4	51800.88	9.45
P10818	Cytochrome c oxidase polypeptide 6A1, mitochondrial	9665.85	6.35
P35738	2-oxoisovalerate dehydrogenase subunit beta, mitochondrial	37808.41	5.33
P38718	Brain protein 44	14257.91	10.49
P38983	40 S ribosomal protein SA	32692.86	4.80
P42930	Heat shock protein beta-1	22892.67	6.12
P48679	Lamin-A	73992.27	6.54
P61983	14-3-3 protein gamma	28302.59	4.80
P62959	Histidine triad nucleotide-binding protein 1	13645.71	6.39
P70567	Tropomodulin-1	40480.07	4.97
Q499N5	Acyl-CoA synthetase family member 2, mitochondrial	62627.20	6.87
P08010	Glutathione S-transferase Mu 2	25571.43	7.31
P08932	T-kininogen 2	45723.55	5.76
P50399	Rab GDP dissociation inhibitor beta	50537.13	5.93
P60711	Actin, cytoplasmic 2	41736.73	5.29
Q03626	Murinoglobulin-1	162631.90	5.62
P36201	Cysteine-rich protein 2	22695.97	8.94
Q5RKI0	WD repeat-containing protein 1	66050.26	6.15
P05506	NADH-ubiquinone oxidoreductase chain 3	13070.54	4.38
P15865	Histone H1.2	21856.16	11.10
P28480	T-complex protein 1 subunit alpha	60359.65	5.86
P13471	40S ribosomal protein S14	16127.49	10.08
P05544	Serine protease inhibitor A3L	43500.79	5.59
P09006	Serine protease inhibitor A3N	43574.12	5.63
P21396	Amine oxidase [flavin-containing] A	59507.83	8.12
P25113	Phosphoglycerate mutase 1	28700.79	6.75
P20761	Ig gamma-2B chain C region		
P04639	Apolipoprotein A-I	27368.91	5.51
Q4G069	Regulator of microtubule dynamics protein 1	35400.55	7.60
P69527	Aminopeptidase O	92836.98	6.12
P02764	Alpha-1-acid glycoprotein	21630.66	5.70
P97532	3-mercaptopyruvate sulfurtransferase	32940.20	5.88
O09175	Aminopeptidase B	72488.67	5.47
P06214	Delta-aminolevulinic acid dehydratase	36031.59	6.31
P13635	Ceruloplasmin	118667.02	5.30
P14669	Annexin A3	36363.20	5.96
P24473	Glutathione S-transferase kappa 1	25361.77	9.13
P30904	Macrophage migration inhibitory factor	12346.05	7.28
P53987	Monocarboxylate transporter 1	53238.22	8.62
P62076	Mitochondrial import inner membrane translocase subunit Tim13	10457.94	8.42
P63029	Translationally-controlled tumor protein	19462.17	4.76
P85515	Alpha-centractin	42613.74	6.19
P97576	GrpE protein homolog 1, mitochondrial	21292.33	6.12

Q01129	Decorin	36363.99	9.06
Q5I0P2	Glycine cleavage system H protein, mitochondrial	13784.41	4.42
Q5XHZ0	Heat shock protein 75 kDa, mitochondrial	73943.52	5.91
Q62930	Complement component C9	60279.30	5.60
Q6P7Q4	Lactoylglutathione lyase	20688.42	5.12
Q9WUS0	Adenylate kinase isoenzyme 4, mitochondrial	25202.92	7.80
P85973	Purine nucleoside phosphorylase	32301.93	6.46
Q9QYE7	Integrin alpha-D	124731.98	5.72
P09456	cAMP-dependent protein kinase type I-alpha regulatory subunit	43094.98	5.27
Q62688	Inactive phospholipase C-like protein 1	122772.40	5.47
Q9WV75	Spondin-2	33273.41	5.59
P19332	Microtubule-associated protein tau	78432.81	5.95
P61589	Transforming protein RhoA	21442.68	5.83
P67999	Ribosomal protein S6 kinase beta-1	59131.52	6.35
Q9QW07	1-phosphatidylinositol-4,5-bisphosphate phosphodiesterase beta-4	134365.47	6.42
Q5PQS7	Uncharacterized protein C3orf19 homolog	54449.15	6.13
O54735	cGMP-specific 3',5'-cyclic phosphodiesterase	94556.18	5.74
O35878	Heat shock protein beta-2	20346.67	5.27
P85108	Tubulin beta-2B chain	49906.97	4.78
Q5I0C3	Methylcrotonoyl-CoA carboxylase subunit alpha, mitochondrial	74908.39	6.21
P0C2X9	Delta-1-pyrroline-5-carboxylate dehydrogenase, mitochondrial	59186.39	6.26
P51839	Olfactory guanylyl cyclase GC-D	114709.72	6.42
P05504	ATP synthase subunit a	25050.43	9.60
P41562	Isocitrate dehydrogenase [NADP] cytoplasmic	46734.43	6.53
Q5XIE6	3-hydroxyisobutyryl-CoA hydrolase, mitochondrial	39157.11	6.52
P11598	Protein disulfide-isomerase A3	54239.39	5.78
Q8VID1	Dehydrogenase/reductase SDR family member 4	29821.80	9.60
P17209	Myosin light chain 4	21282.18	4.96
P63251	G protein-activated inward rectifier potassium channel 1	56573.28	8.60
P31211	Corticosteroid-binding globulin	42243.07	4.80
P47858	6-phosphofructokinase, muscle type	85428.75	8.23
P62890	60S ribosomal protein L30	12784.05	9.65
Q3T1K5	F-actin-capping protein subunit alpha-2	32835.87	5.58
Q62658	Peptidyl-prolyl cis-trans isomerase FKBP1A	11791.44	8.08
Q6AY09	Heterogeneous nuclear ribonucleoprotein H	49293.60	5.89
Q8VIF7	Selenium-binding protein 1	52532.07	6.10
Q9QY17	Protein kinase C and casein kinase substrate in neurons 2 protein	55977.89	5.04
P18418	Calreticulin	46348.33	4.33
Q6AYL2	Germ cell-specific gene 1 protein	36057.13	5.59
Q9JM59	Kv channel-interacting protein 2	30932.76	4.93
Q9JJ79	Cytoplasmic dynein 2 heavy chain 1	492218.13	6.23
Q6IG02	Keratin, type II cytoskeletal 2 epidermal	69127.04	7.58
Q99PV3	Muskelin	84702.75	5.92
P0C0K7	Ephrin type-B receptor 6	107193.41	6.38
Q68FP1	Gelsolin	83510.51	5.65
P15146	Microtubule-associated protein 2	202410.75	4.77
P08009	Glutathione S-transferase Mu 2	25549.49	7.27
P07335	Creatine kinase B-type	42594.08	5.40
Q6P6V1	Polypeptide N-acetylgalactosaminyltransferase 11	69039.10	8.58

P05708	Hexokinase-1	102408.01	6.29
P21263	Nestin	208797.47	4.30
O54728	Phospholipase B1, membrane-associated	158727.08	6.21
Q9ERB4	Versican core protein (Fragments)	297749.90	4.48
Q704S8	Carnitine O-acetyltransferase	70800.73	8.73
Q6AYT9	Acyl-coenzyme A synthetase ACSM5, mitochondrial	61889.70	6.72
P51650	Succinate-semialdehyde dehydrogenase, mitochondrial	52188.67	6.40
P70470	Acyl-protein thioesterase 1	24708.72	6.04
Q5XFX0	Transgelin-2	22262.22	8.45
Q5XIT9	Methylcrotonoyl-CoA carboxylase beta chain, mitochondrial	59037.20	7.27
Q66HB5	Radial spoke head 10 homolog B	101586.80	6.58
Q8R508	Protocadherin Fat 3	498700.77	4.70
Q9QYV8	DNA polymerase subunit gamma-1	136855.60	6.43
Q6LED0	Histone H3.1	15272.89	11.13
Q5QD51	A-kinase anchor protein 12	180979.01	4.34
Q9Z244	GMP reductase 1	37487.94	6.50
O88422	Polypeptide N-acetylgalactosaminyltransferase 5	105119.63	9.21
Q6UPR8	Endoplasmic reticulum metallopeptidase 1	99896.84	6.82
Q62671	E3 ubiquitin-protein ligase UBR5 (Fragment)	308026.95	5.72
P62828	GTP-binding nuclear protein Ran	24291.91	7.20
Q9JI51	Vesicle transport through interaction with t-SNAREs homolog 1A	26042.71	6.07
P41350	Caveolin-1	20421.41	5.30
Q497B0	Nitrilase homolog 2	30700.99	6.90
P70536	Oxytocin receptor	42868.60	9.56
P61016	Cardiac phospholamban	6094.51	9.15
Q9Z2A6	Mitogen-activated protein kinase 15	60723.56	9.83
Q710E6	Protein C1orf9 homolog	137121.91	4.94
Q535K8	GON-4-like protein	247902.63	4.82
Q8K3U6	Coagulation factor VII	17565.44	5.07
O88831	Calcium/calmodulin-dependent protein kinase kinase 2	64446.26	5.64
P11608	ATP synthase protein 8	7641.97	9.30
Q99N02	Solute carrier organic anion transporter family member 3A1	76825.35	6.77
Q6RFZ7	Pleckstrin homology domain-containing family G member 5	115784.30	6.60
P51579	P2X purinoceptor 6	42450.59	6.45
Q9QZR8	PDZ domain-containing protein 2	293889.82	8.44
Q62667	Major vault protein	95667.05	5.43
Q9JHZ4	GRIP1-associated protein 1	96073.87	5.17
P19492	Glutamate receptor 3	98051.86	8.26
Q4V8H8	EH domain-containing protein 2	61237.48	6.12
Q62936	Disks large homolog 3	93539.44	6.32
Q5M965	Probable tRNA (His) guanylyltransferase	34849.81	8.44
Q07014	Tyrosine-protein kinase Lyn	58528.91	6.76
O54889	DNA-directed RNA polymerase I subunit RPA1	194192.16	6.43
Q62724	DNA replication licensing factor MCM6 (Fragment)		
P35565	Calnexin	65129.16	4.48
P30427	Plectin-1	533540.00	5.71
P10817	Cytochrome c oxidase polypeptide 6A2, mitochondrial (Fragment)	9474.69	8.13
Q3MIB4	Peroxisomal Lon protease homolog 2	94393.20	6.77
P97526	Neurofibromin	316952.26	6.96

P52590	Nuclear pore complex protein Nup107	107208.89	5.34
Q3KRC5	tRNA-dihydrouridine synthase 3-like	71408.75	7.79
P15389	Sodium channel protein type 5 subunit alpha	227367.25	5.47
P23562	Band 3 anion transport protein	103172.71	5.28
Q5BK10	Calpain-13	76938.62	6.49
P30823	High affinity cationic amino acid transporter 1	67267.11	5.73
P16221	Cytochrome c oxidase polypeptide 8H, mitochondrial	4765.54	9.53
P20070	NADH-cytochrome b5 reductase 3	34043.44	8.57
P35467	Protein S100-A1	10428.65	4.37
P50398	Rab GDP dissociation inhibitor alpha	50536.64	5.00
Q7M0E3	Destrin	18402.40	8.24
P29995	Inositol 1, 4, 5-trisphosphate receptor type 2	307058.38	6.06
P0C0R5	Phosphoinositide 3-kinase regulatory subunit 4	152315.53	6.76
Q6ED65	Echinoderm microtubule-associated protein-like 5	219807.68	8.00
Q7TT49	Serine/threonine-protein kinase MRCK beta	194887.69	6.05
Q03343	Adenylate cyclase type 6	130506.35	8.49
Q5XIA3	Leucine carboxyl methyltransferase 2	75532.60	6.54
Q3T1G7	Conserved oligomeric Golgi complex subunit 7	86211.84	5.24
P49621	Diacylglycerol kinase beta	90287.96	8.30
Q6IE52	Murinoglobulin-2	158868.77	6.12
P35365	5-hydroxytryptamine receptor 5B	41122.28	9.83
P50137	Transketolase	67643.64	7.22
Q5U300	Ubiquitin-like modifier-activating enzyme 1	117787.78	5.36
Q63618	Espin	90568.83	6.68
Q9JIR0	Peripheral-type benzodiazepine receptor-associated protein 1	200203.54	5.17
P05505	Cytochrome c oxidase subunit 3	29739.51	6.59
Q9JK11	Reticulon-4	126388.09	4.41
P05426	60S ribosomal protein L7	30329.26	10.87
O89040	1-phosphatidylinositol-4,5-bisphosphate phosphodiesterase beta-2	134882.94	5.81
P37199	Nuclear pore complex protein Nup155	155002.84	5.84
O54766	Zona pellucida sperm-binding protein 1	57997.92	6.23
Q8K4V4	Sorting nexin-27	61014.88	5.95
P19132	Ferritin heavy chain	21126.66	5.86
Q7TNK6	tRNA guanosine-2'-O-methyltransferase TRM11 homolog	53102.77	8.02
Q99J82	Integrin-linked protein kinase	51373.17	8.30
O35567	Bifunctional purine biosynthesis protein PURH	64208.42	6.69
Q9WV48	SH3 and multiple ankyrin repeat domains protein 1	226335.15	8.52
Q63148	Chordin	99459.77	7.26
Q62929	Interleukin-1 receptor-like 2	61820.83	7.03
P97571	Calpain-1 catalytic subunit	81988.04	5.46
Q5XI06	Probable histone acetyltransferase MYST1	52500.84	8.59
P11497	Acetyl-CoA carboxylase 1	265193.51	5.97
Q99PD6	Transforming growth factor beta-1-induced transcript 1 protein	50122.60	6.49
Q3SWT6	Serine/threonine-protein phosphatase with EF-hands 1	73966.47	6.65
P11950	Cytochrome c oxidase polypeptide VIc-2	8421.85	10.07
Q9R1J8	Prolyl 3-hydroxylase 1	81147.05	5.00
Q3T1I3	USH1C-binding protein 1	74611.76	5.41
O54975	Xaa-Pro aminopeptidase 1	69657.53	5.38

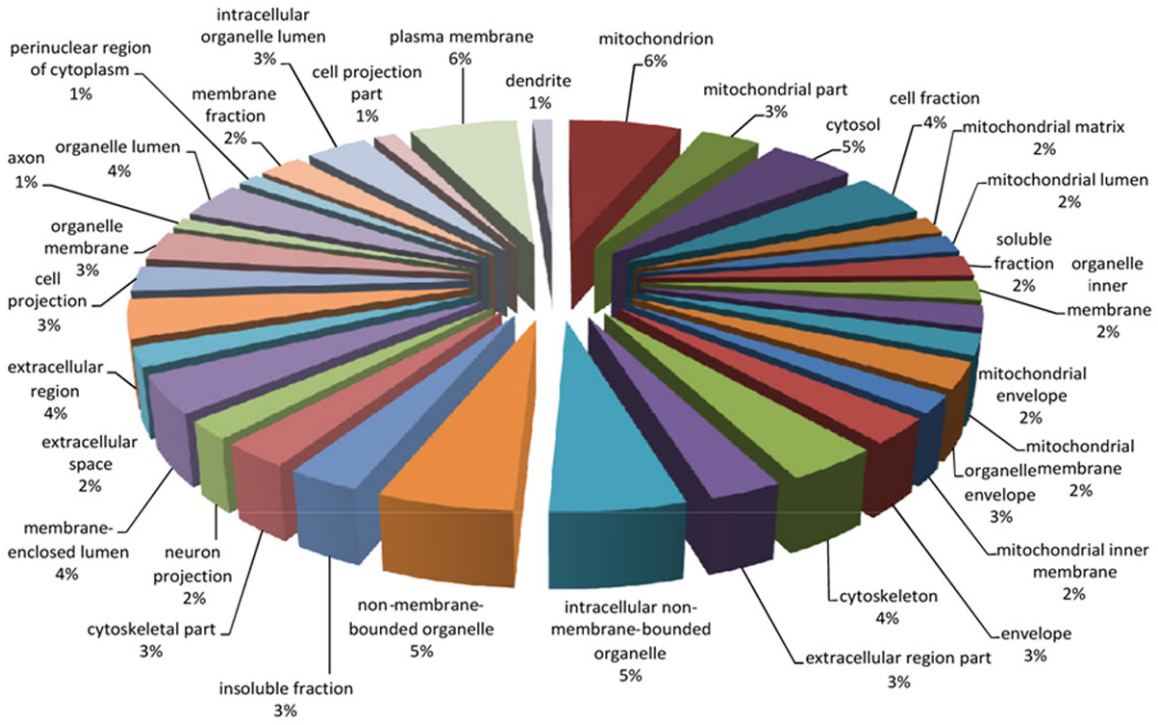

Figure 2. Functional classification of proteomics data by bioinformatics analysis. The cellular component categories according to bioinformatics analysis. Categorizations are based on information provided by the online resource Gene Ontology and DAVID Bio-informatics Resources.

were involved in response to organic substance, macromolecular complex subunit organization and macromolecular complex assembly (**Figure 4**).

Network of the differential proteins change >2.0-fold

All the differential proteins change >2.0-fold were uploaded into the STRING 9.0 software to analyze the interactions of all the proteins. As shown in **Figure 5**, 24 hours after hypoxia and ischemia, some important modulators in energy metabolism including ATP synthase subunit e(Atp5i), ATP synthase subunit a (ATP6) and ATP synthase protein 8 (ATP8) et al. seemed to be activated which interacted with numerous different proteins. In addition, dihydrolipoyllysine-residue succinyltransferase component of 2-oxoglutarate dehydrogenase complex (Dlst), cytochrome c oxidase subunit 3 (Cox3), isocitrate dehydrogenase [NAD] subunit beta (Idh3B), superoxide dismutase (Sod2), et al. were found to be interacted with quite a lot of proteins. Most of the proteins mentioned above were enzymes involved in biochemical process. Besides, some important proteins participated in neuron projection or axon related process including microtubule-associated protein 2 (map2), microtubule-associated protein tau (mapt) and calnexin (canx) et al. were all interacted with several differential proteins detected in our study. All of these mentioned above constituted a complex network.

Increased expression of MAP-2 and MAPT (Tau) after hypoxic-ischemic *brain damage*

Among the differential expressed proteins, some important proteins participated in neuron projection or axon related process such as microtubule-associated protein 2 (MAP-2) and microtubule-associated protein tau (MAPT) et al. According to our study, both of these proteins are expressed only in hypoxic-ischemic brain injury group. We then used Western blot to verify the fold changes of MAP-2 and MAPT mentioned above. MAP-2 is one of the most important cytoskeleton proteins which is predominantly expressed in dendrites of neurons [21]. Tau promotes microtubule assembly and stability, and might be involved in the establishment and maintenance of neuronal polarity. The C-terminus binds axonal microtubules while the N-terminus binds neural plasma membrane components, suggesting that tau

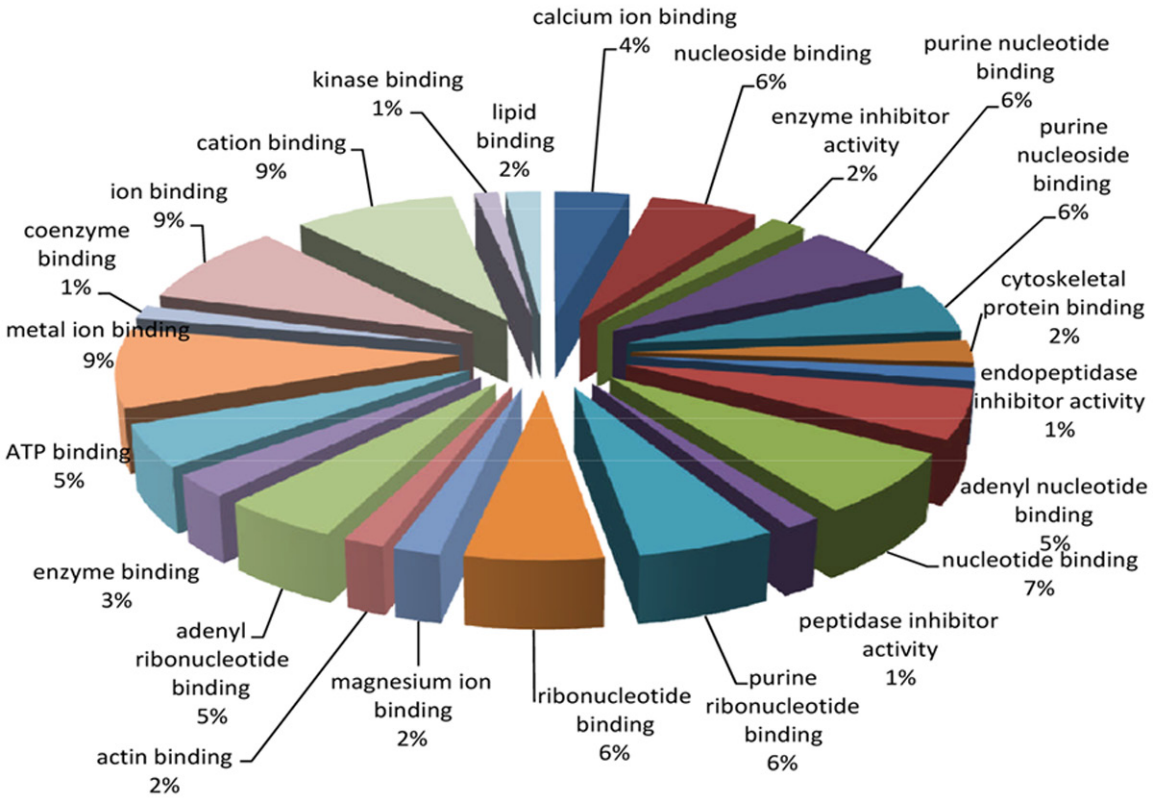

Figure 3. The molecular function categories by gene number according to bioinformatics analysis. Categorizations are based on information provided by the online resource Gene Ontology and DAVID Bio-informatics Resources.

functions as a linker protein between both. Axonal polarity is predetermined by tau localization (in the neuronal cell) in the domain of the cell body defined by the centrosome. Results of Western blot showed that a nearly 2.15-fold change was detected for MAP-2 and 2.13-fold change was detected for Tau (**Figure 6**). The results were coincident with proteomic analysis.

Discussion

To improve the survival rate and quality of life in premature infants is one of the key objectives of neonatal medicine in this century. According to WHO, there are 15000000 preterm births worldwide every year, and the incidence of premature infants is increasing year by year [22]. The number of premature infants born with hypoxic ischemic brain injury is even more amazing in China. Learning difficulties often occur in preterm infants including reading, spelling, calculation or writing difficulties [23]. Although the prognosis of preterm infants has been greatly improved in recent years, the sequelae of brain injury in preterm infants is still a serious problem affecting the quality of life. Perinatal and neonatal scientific development greatly improves the survival rate of premature infants, but the incidence rate of injury in preterm infants hypoxic ischemia brain did not reduce. This is because of the better survival of extremely preterm infants who are more susceptible to hypoxia ischemia brain injury [24]. Therapeutic strategies to prevent or reduce the long-term effects of hypoxic-ischemic brain damage (HIBD) are limited to date. However, the details of the mechanism leading to long-term and permanent brain damage induced by hypoxia-ischemia have not yet been fully elucidated. Proteomics can analyze protein expression at the general level and thus could provide insight into the potential unknown mechanism. Furthermore, fully elucidated details in brain damage after hypoxia and ischemia attack may allow development of neuroprotective therapies.

In this study, we established hypoxia-ischemia brain damage using SD neonatal rats at the 3rd

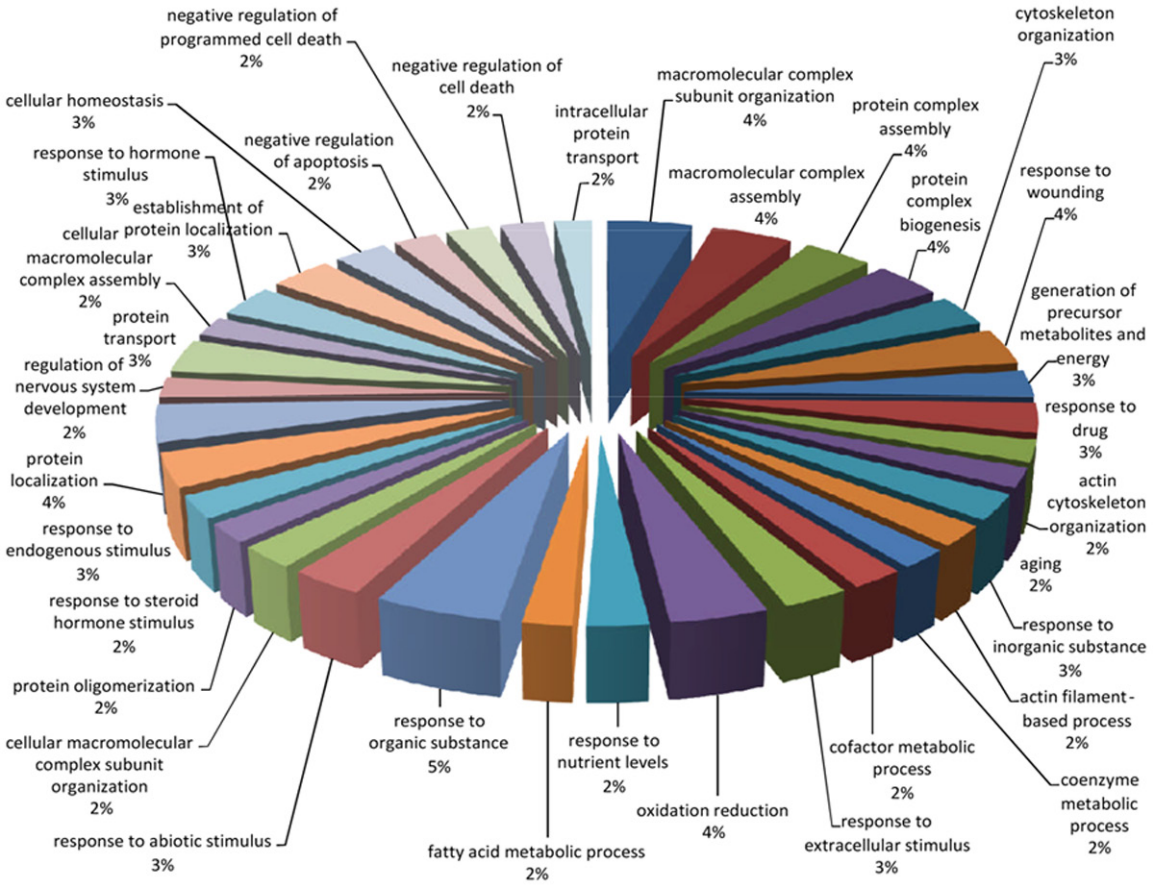

Figure 4. The biological process categories according to bioinformatics analysis. Categorizations are based on information provided by the online resource Gene Ontology and DAVID Bio-informatics Resources.

postnatal day (P3) to mimics hypoxic-ischemic event in preterm infants, since brain development of rats at P3 present similar to that of human preterm infants between 24 to 28 weeks of gestation [17, 18].

We used label-free quantitative shotgun proteomic method to investigate the proteins differentially expressed when hypoxia-ischemia brain damage happened for 24 hours. According to the results, we could see that 34 protein were more than 2-fold up-regulated and 14 protein were more than 2-fold down-regulated in hypoxia-ischemia group, while 193 proteins were present only in hypoxia-ischemia group. In the first 24 hours, there were so many proteins dramatically changed but we had no idea what category they belonged to. Classification of these proteins using Gene Ontology database showed that the majority of differentially expressed proteins comprised mitochondrial proteins, plasma membrane proteins, and non-membrane-bounded organelle et al. These results indicated that during the first 24 hours after hypoxia-ischemia attack, membrane and organelles reacted quickly and sensitively. And these also indicated that proteins of plasma membrane and organelle were more susceptible to hypoxia and ischemia assault.

DAVID classification of proteins by molecular function revealed that the majority of proteins were involved in ion binding, energy metabolism, cytoskeletal and structural molecule activity and enzyme regulation et al. The activation of energy metabolism and enzymes leads to a series of follow-up process. As we all know, a decreased core body temperature is known to affect kinetic properties of many enzyme systems [25]. That is why therapeutic hypothermia is still the most potent neuroprotective strategy to date [26].

DAVID classification of proteins by biological process showed that the majority of proteins

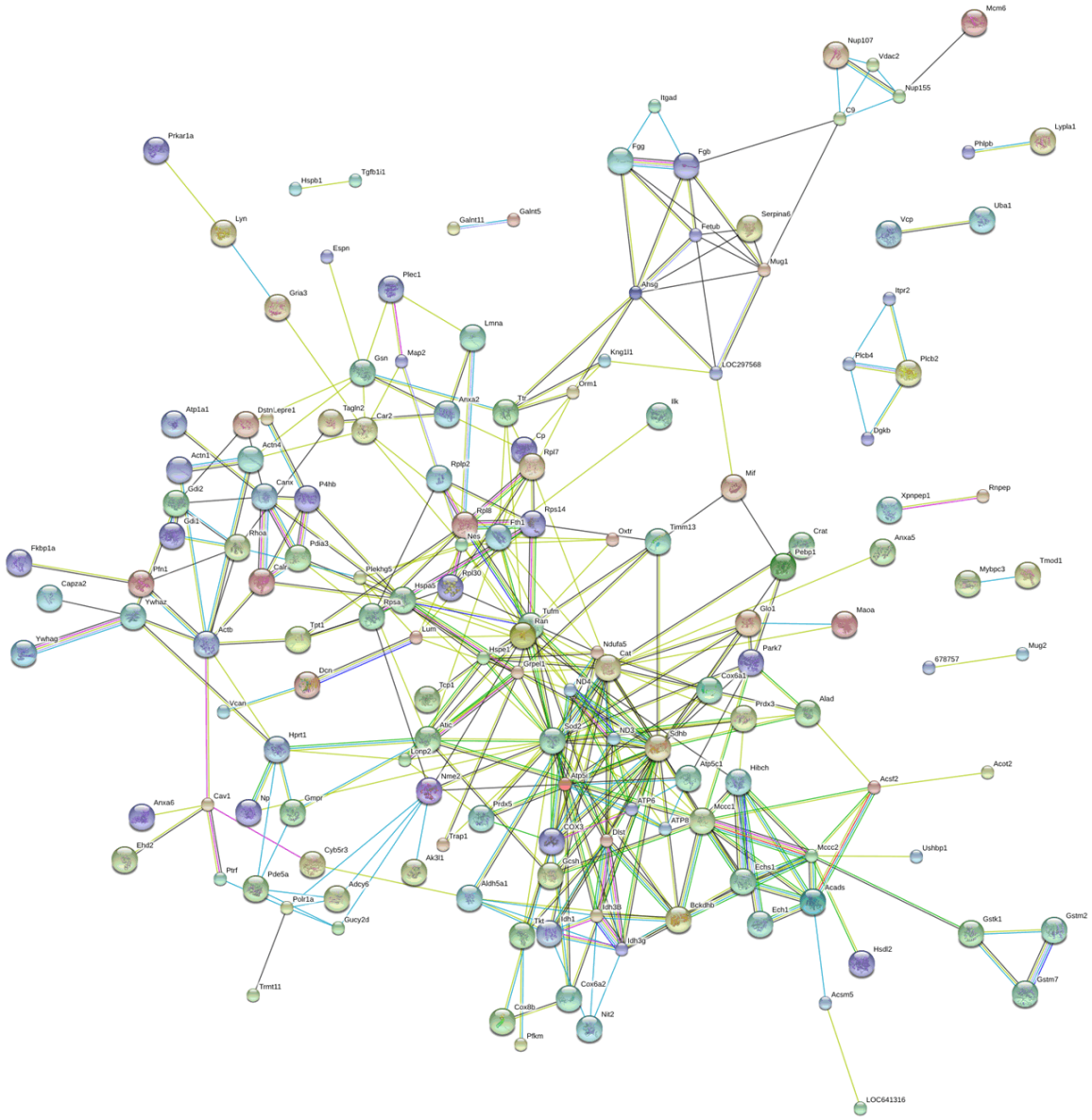

Figure 5. The network analysis of proteins differentiated expressed in hypoxia-ischemia group using STRING 9. All the differential proteins change >2.0-fold were uploaded into the STRING 9.0 software to analyze the interactions of all the proteins. Color ball: the changed protein; yellow line: text mining; purple line: experiments; blue line: databases; light blue: homology; black line: coexpression; green line: neighborhood; red line, gene fusion; deep blue: cooccurrence.

were involved in response to organic substance, macromolecular complex and protein complex assembly and localization, oxidation and reduction, response to wounding, response to endogenous stimulus, homeostatic process et al. Besides, some reactions such like ion transport, cytoskeleton organization, apoptosis and cell death et al. are also involved.

After analysis of differential expressed proteins using STRING 9.0 software, we found that most differential expressed proteins interacted each other more or less (**Figure 3**). Within this complex network, the proteins with most relationship to others are almost enzymes. Besides, the two proteins we chose to verify using Western blot, MAP-2 and Tau, participated in neuron projection or axon related process.

MAP-2 is not only a structural component of neurons, but also participates in the repair process of neuronal growth and injury. Most stud-

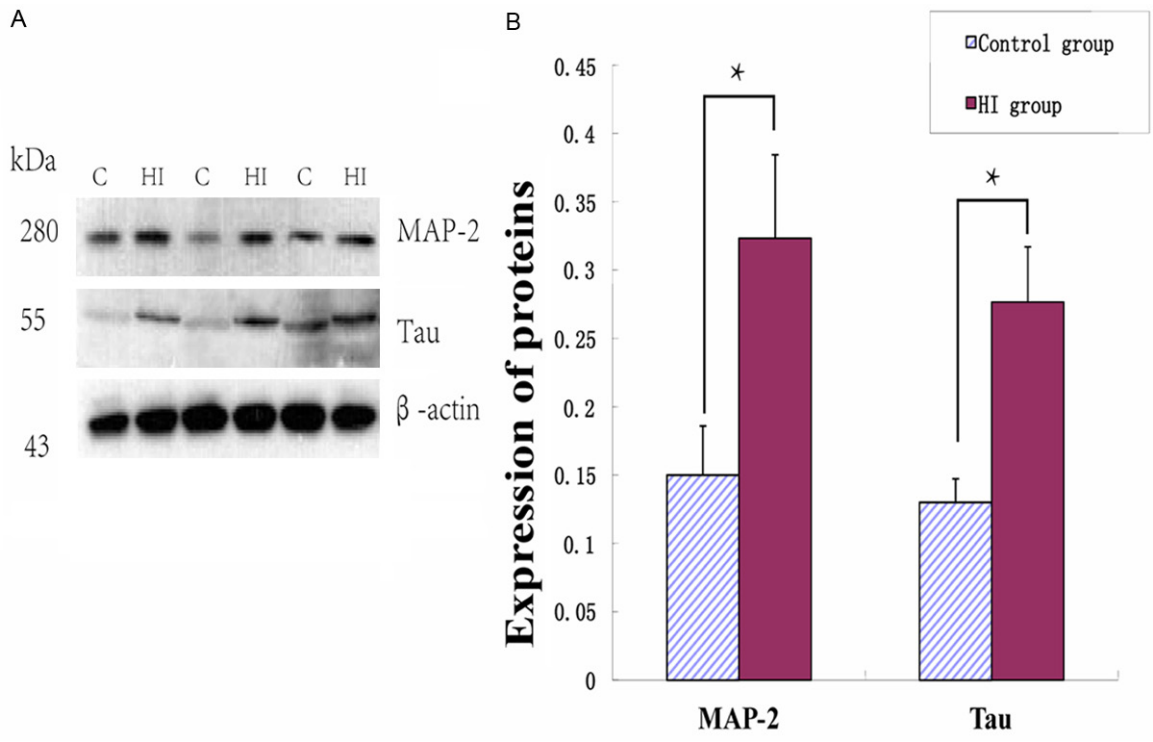

Figure 6. Changes in the protein expression of MAP-2 and Tau determined by Western blot analysis. Expression of MAP-2 was up-regulated in hypoxia ischemia group compared with control group (fold change = 2.15). Expression of Tau was up-regulated in hypoxia ischemia group compared with control group (fold change = 2.13). Expression of β-actin was used as a loading control.

ies showed there was increased expression of MAP-2 after transient ischemia which might suggests that the tolerance to ischemia was increased. However, the expression of MAP-2 declined gradually with the death of neurons [27, 28]. MAP-2 expression is high in the early stage after brain lesion, probably due to compensatory regeneration [29], and low in later stage after ischemia [30]. The increase of the MAP-2 expression also occurs in a neural organization induced by exercise after cerebral ischemia [31] or cerebral physiological conditions [32]. MAP-2 also regulates neuronal polarity and dendritic extension, and it promotes structure modulation and morphological stabilization in neuronal cells [33]. Physically, Tau protein can promote formation of microtubule and maintain the stability of microtubules formed. Numerous studies reported Tau involved in Alzheimer's disease and one of hypothesis of AD was that the phosphorylation of Tau would ultimately lead to AD. One study reported that a tau transgenic mouse model overexpressing human 4R1N double-mutant tau and that develops AD (Alzheimer's disease)-like NFTs (neurofibrillary tangles) in an age-dependent manner [34].

In short, we had carried out a full-scale screening of the proteomics after hypoxia-ischemia damage for 24 hours. Based on this study, we found 193 proteins were present only in hypoxia-ischemia group, 34 protein were more than 2-fold up-regulated and 14 protein were more than 2-fold down-regulated in hypoxia-ischemia group determined by liquid chromatography-mass spectrometry/mass spectrometry. All the proteins mentioned above involved in ion binding, energy metabolism, cytoskeletal and structural molecule activity and enzyme regulation et al. These differentially expressed proteins might serve as valuable biomarkers that might predict the presence of a precursor field and need to be further investigated.

Acknowledgements

This work is supported by grants from the National Science Foundation of China (No. 81370741); Beijing Natural Science Foundation (No. 7122045); The Natural Science Foundation

of Beijing City and Beijing City Board of Education Science and Technology Project (KZ201410025025).

Disclosure of conflict of interest

None.

Address correspondence to: Dr. Hong Cui, Department of Pediatrics, Beijing Friendship Hospital, Capital Medical University, 95 Yong'an Road, Xi'cheng District, Beijing 100050, China. Tel: +86 010-63139763; E-mail: cuihong100@sina.com

References

[1] Northington FJ, Ferriero DM, Martin LJ. Neurodegeneration in the thalamus following neonatal hypoxia-ischemia is programmed cell death. Dev Neurosci 2001; 23: 186-191.

[2] Hermans RH, Hunter DE, McGivern RF, Cain CD, Longo LD. Behavioral sequelae in young rats of acute intermittent antenatal hypoxia. Neurotoxicol Teratol 1992; 14: 119-129.

[3] Pazaiti A, Soubasi V, Spandou E, Karkavelas G, Georgiou T, Karalis P, Guiba-Tziampiri O. Evaluation of long-lasting sensorimotor consequences following neonatal hypoxic-ischemic brain injury in rats: the neuroprotective role of MgSO4. Neonatology 2009; 95: 33-40.

[4] Fan X, van Bel F, van der Kooij MA, Heijnen CJ, Groenendaal F. Hypothermia and erythropoietin for neuroprotection after neonatal brain damage. Pediatr Res 2013; 73: 18-23.

[5] Wu YW, Bauer LA, Ballard RA, Ferriero DM, Glidden DV, Mayock DE, Chang T, Durand DJ, Song D, Bonifacio SL, Gonzalez FF, Glass HC, Juul SE. Erythropoietin for neuroprotection in neonatal encephalopathy: safety and pharmacokinetics. Pediatrics 2012; 130: 683-691.

[6] Liu W, Shen Y, Plane JM, Pleasure DE, Deng W. Neuroprotective potential of erythropoietin and its derivative carbamylated erythropoietin in periventricular leukomalacia. Exp Neurol 2011; 230: 227-239.

[7] Zhou Y, Lekic T, Fathali N, Ostrowski RP, Martin RD, Tang J, Zhang JH. Isoflurane posttreatment reduces neonatal hypoxic-ischemic brain injury in rats by the sphingosine-1-phosphate/phosphatidylinositol-3-kinase/Akt pathway. Stroke 2010; 41: 1521-1527.

[8] McAuliffe JJ, Loepke AW, Miles L, Joseph B, Hughes E, Vorhees CV. Desflurane, isoflurane, and sevoflurane provide limited neuroprotection against neonatal hypoxia-ischemia in a delayed preconditioning paradigm. Anesthesiology 2009; 111: 533-546.

[9] Zhao P, Peng L, Li L, Xu X, Zuo Z. Isoflurane preconditioning improves long-term neurologic outcome after hypoxic-ischemic brain injury in neonatal rats. Anesthesiology 2007; 107: 963-70.

[10] Zuo Z, Wang Y, Huang Y. Isoflurane preconditioning protects human neuroblastoma SH-SY5Y cells against in vitro simulated ischemia-reperfusion through the activation of extracellular signal-regulated kinases pathway. Eur J Pharmacol 2006; 542: 84-91.

[11] Hammerman C, Kaplan M. Ischemia and reperfusion injury. The ultimate pathophysiologic paradox. Clin Perinatol 1998; 25: 757-777.

[12] Inder TE, Volpe JJ. Mechanisms of perinatal brain injury. Semin Neonatol 2000; 5: 3-16.

[13] Verklan MT. The chilling details: hypoxic-ischemic encephalopathy. J Perinat Neonatal Nurs 2009; 23: 59-68.

[14] Fatemi A, Wilson MA, Johnston MV. Hypoxic-ischemic encephalopathy in the term infant. Clin Perinatol 2009; 36: 835-858.

[15] Distefano G, Praticò AD. Actualities on molecular pathogenesis and repairing processes of cerebral damage in perinatal hypoxic-ischemic encephalopathy. Ital J Pediatr 2010; 36: 63.

[16] Donega V, van Velthoven CT, Nijboer CH, van Bel F, Kas MJ, Kavelaars A, Heijnen CJ. Intranasal mesenchymal stem cell treatment for neonatal brain damage: long-term cognitive and sensorimotor improvement. PLoS One 2013; 8: e51253.

[17] Carty ML, Wixey JA, Kesby J, Reinebrant HE, Colditz PB, Gobe G, Buller KM. Long-term losses of amygdala corticotropin-releasing factor neurons are associated with behavioural outcomes following neonatal hypoxia-ischemia. Behav Brain Res 2010; 208: 609-18.

[18] Stadlin A, James A, Fiscus R. Development of a postnatal 3-day-old rat model of mild hypoxic-ischemic brain injury. Brain Res 2003; 993: 101-110.

[19] Zhu W, Smith JW, Huang CM. Mass spectrometry-based label-free quantitative proteomics. J Biomed Biotechnol 2010; 2010: 840518.

[20] Liu Y, Xue F, Liu G, Shi X, Liu Y, Liu W, Luo X, Sun X, Kang Z. Helium preconditioning attenuates hypoxia/ischemia-induced injury in the developing brain. Brain Res 2011; 1376: 122-129.

[21] Di Stefano G, Casoli T, Fattoretti P, Balietti M, Grossi Y, Giorgetti B, Bertoni-Freddari C. Level and distribution of microtubule-associated protein-2 (MAP2) as an index of dendritic structural dynamics. Rejuvenation Res 2006; 9: 94-98.

[22] Blencowe H, Cousens S, Oestergaard MZ, Chou D, Moller AB, Narwal R, Adler A, Vera Garcia C, Rohde S, Say L, Lawn JE. National, regional, and worldwide estimates of preterm birth rates in the year 2010 with time trends

since 1990 for selected countries: a systematic analysis and implications. Lancet 2012; 379: 2162-2172.
[23] Carla A, D'Argenzio L, Ticconi C, Di Paolo A, Stellin V, Lopez L, Curatolo P. Brain damage in preterm infants: etiological phways. Ann Ist Super Sanita 2005; 41: 229-237.
[24] Bonifacio SL, Glass HC, Peloquin S, Ferriero DM. A new neurological focus in neonatal intensive care. Nat Rev Neurol 2011; 7: 485-494.
[25] Tocco NM, Hodge AE, Jones AA, Wispe JR, Valentine CJ. Neonatal therapeutic hypothermia-associated hypomagnesemia during parenteral nutrition therapy. Nutr Clin Pract 2014; 29: 246-248.
[26] Wu TC, Grotta JC. Hypothermia for acute is chaemic stroke. Lancet Neurol 2013; 12: 275-284.
[27] Rota Nodari L, Ferrari D, Giani F, Bossi M, Rodriguez-Menendez V, Tredici G, Delia D, Vescovi AL, De Filippis L. Long-term survival of human neural stem cells in the ischemic rat brain upon transient immunosuppression. PLoS One 2010; 5: e14035.
[28] Zhou Q, Zhang Q, Zhao X, Duan YY, Lu Y, Li C, Li T. Cortical electrical stimulation alone enhances functional recovery and dendritic structures after focal cerebral ischemia in rats. Brain Res 2010; 1311: 148-157.
[29] Iglesias S, Marchal G, Viader F, Baron JC. Delayed intrahemispheric remote hypometabolism: correlations with early recovery after stroke. Cerebrovasc Dis 2000; 10: 391-402.
[30] Wang F, Xing S, He M, Hou Q, Chen S, Zou X, Pei Z, Zeng J. Nogo-A is associated with secondary degeneration of substantia nigra in hypertensive rats with focal cortical infarction. Brain Res 2012; 1469: 153-163.
[31] Derksen MJ, Ward NL, Hartle KD, Ivanco TL. MAP2 and synaptophysin protein expression following motor learning suggests dynamic regulation and distinct alterations coinciding with synaptogenesis. Neurobiol Learn Mem 2007; 87: 404-415.
[32] Garcia PC, Real CC, Ferreira AF, Alouche SR, Britto LR, Pires RS. Different protocols of physical exercise produce different effects on synaptic and structural proteins in motor areas of the rat brain. Brain Res 2012; 1456: 36-48.
[33] Poulain FE, Sobel A. The microtubule network and neuronal morphogenesis: dynamic and coordinated orchestration through multiple players. Mol Cell Neurosci 2010; 43: 15-32.
[34] Ando K, Leroy K, Heraud C, Kabova A, Yilmaz Z, Authelet M, Suain V, De Decker R, Brion JP. Deletion of murine tau gene increases tau aggregation in a human mutant tau transgenic mouse model. Biochem Soc Trans 2010; 38: 1001-1005.